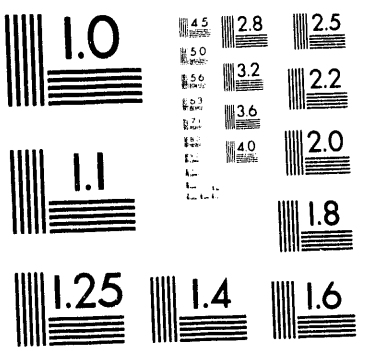
1.0
1.1
1.25
1.4
1.6
1.8
2.0
2.2
2.5
2.8
3.2
3.6
4.0
4.5
5.0
5.6

1 of 1

Conf-930173--12

UCRL-JC-112925
PREPRINT

SEP 15 1993
OSTI

Target Rapidity Baryon Distributions in $^{28}Si + ^{197}Au$ and $^{197}Au + ^{197}Au$ Collisions at 14.6 and 11.7 A·GeV/c

T. C. Sangster, J. B. Costales and M. N. Namboodiri
Lawrence Livermore National Laboratory

This article was prepared for submittal to the
Conference Proceedings for HIPAGS93 held at the
Massachusetts Institute of Technology in
Boston, Massachusetts on January 13–15, 1993

February 25, 1993

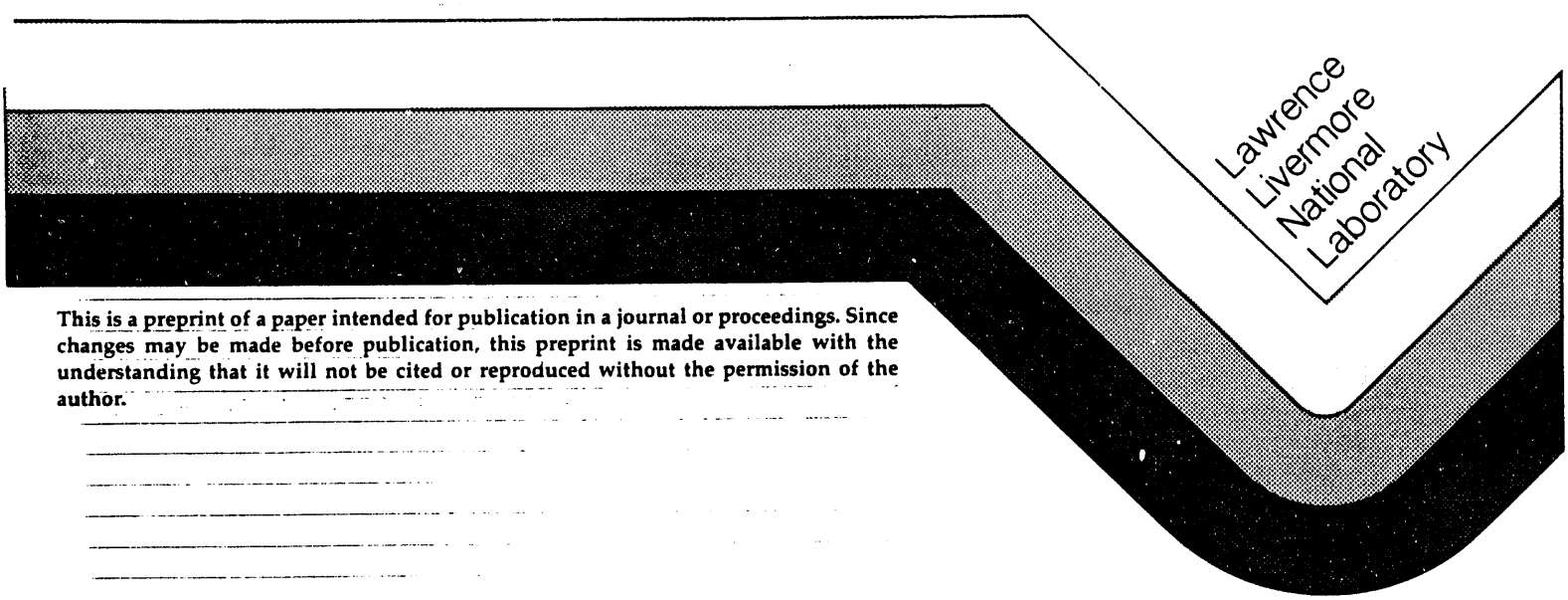

Target Rapidity Baryon Distributions in ^{28}Si +^{197}Au and ^{197}Au +^{197}Au Collisions at 14.6 and 11.7 A·GeV/c

T. C. Sangster, J. B. Costales and M. N. Namboodiri
Lawrence Livermore National Laboratory
P.O. Box 808, Livermore, CA 94550, USA

for Experiment 859 (E802 Collaboration):
ANL–BNL–UCBerkeley–UCRiverside–Columbia–Hiroshima–INS–
Kyushu–LLNL–MIT–NYU–Tokyo

ABSTRACT

Proton and deuteron kinetic energy spectra have been measured at target rapidities for both minimum bias and central collisions of 14.6 A·GeV/c ^{28}Si and 11.7 A·GeV/c ^{197}Au beams with a ^{197}Au target. The spectra were measured from a low energy threshold of approximately E_{kin}=35 MeV to well over 200 MeV for laboratory angles of 50° to 130° ($|\eta| \leq 0.76$). The acceptance–corrected spectra have been fit over a limited range of kinetic energies using a Boltzmann distribution. The integrated yields and the inverse slope parameters are presented as a function of centrality for the ^{28}Si +^{197}Au reaction and as a function of trigger for the ^{197}Au +^{197}Au reaction. These quantities are also compared with the proton spectra generated using both the ARC[1] and RQMD[2] codes.

1. Introduction

Experiment 802[3] at the Brookhaven National Laboratory (BNL) Alternating Gradient Synchrotron (AGS) has measured charged particle distributions (including p, d, $\overline{p}$, $\pi^{\pm}$ and $K^{\pm}$) over a broad range of rapidity ($0.5 \leq y \leq 2.5$) and transverse momentum ($0.2 \leq p_{\perp} \leq 2.5$ GeV/c) for a variety of projectile–target combinations[4,5]. The addition of the E859 Phoswich Array[6] to the E802 apparatus extends the original measurement for protons, deuterons and tritons down to a pseudo–rapidity of η=–0.76, where $\eta \equiv -\log(\tan\theta/2)$. In this paper, we present preliminary results for proton and deuteron emission in 14.6 A·GeV/c ^{28}Si +^{197}Au and 11.7 A·GeV/c ^{197}Au +^{197}Au collisions at pseudo–rapidities of $|\eta| \leq 0.76$ and kinetic energies from approximately 35 to 200 MeV (260 to 650 MeV/c). Since protons measured beyond $\theta \sim 90°$ cannot be emitted in free nucleon–nucleon collisions, these results are a measure of collective multiparticle or multistrp processes and, as such, will serve to constrain and quantify these processes in the dynamical models used to understand the formation and decay of hot, dense nuclear matter.

2. Experimenal Apparatus

The E859 Phoswich Array consists of 42 ΔE–E scintillating plastic telescopes which measure charged particle kinetic energy and provide particle identification (PID) for protons, deuterons and tritons. Although charged pions can be identified, the limited kinetic

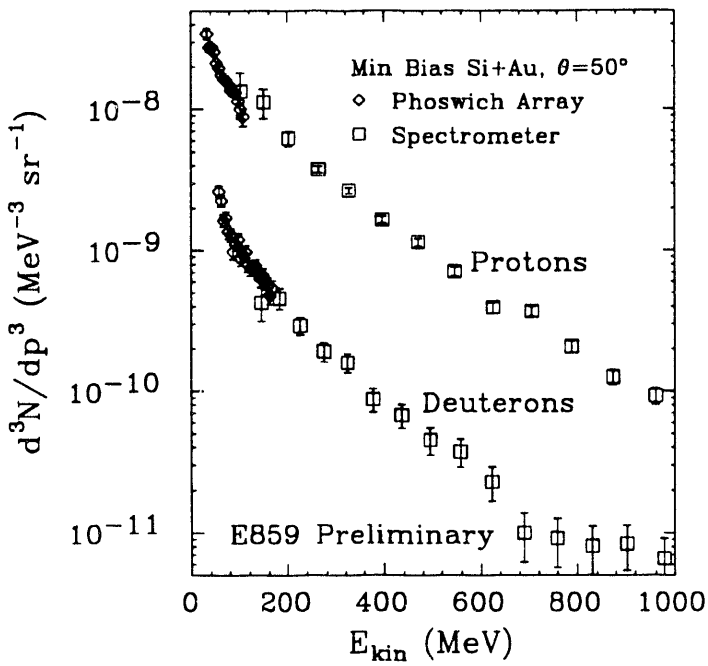

Fig. 1: A comparison of proton and deuteron spectra from the E859 Phoswich Array and the E802 Spectrometer for minimum bias triggers at a laboratory angle of 50°.

energy information does not provide adequate spectra for analysis (pions punch through the plastic modules for $E_{kin} \geq$70 MeV). In addition, $e^{\pm}$'s, n's and γ's each generate some signal. However, these signals are not generally useful for PID and only serve as a measure of the overall hit density or occupancy.

Each of the plastic telescopes consists of a relatively thin layer (5.0 mm thick) of *fast* BC412 (τ_{rise}=1.0 ns, τ_{decay}=3.3 ns) laminated onto the front of a thick block (26.0 cm deep) of *slow* BC444 ($\tau_{rise} \approx$19.5 ns, $\tau_{decay} \approx$260 ns) and readout with a single photomultiplier tube (PMT). By integrating the single PMT signal in both a short (60 ns) and a long (200 ns) ADC gate[7], it is possible to extract quantities which are proportional to the differential energy loss in the fast plastic (ΔE) and residual energy deposited in the slow (E_{res}). Particle identification is then simply a matter of identifying charge or mass bands, according to the Bethe–Bloch relation, in a plot of ΔE–E, where E=ΔE+E_{res} (note that multiple particles in a single phoswich module will generally obscure all PID). In addition, the relatively fast signal from the BC412 provides a time–of–flight ($\sigma \sim$400 ps) which may also be used for PID (primarily for proton–pion separation above E_{kin}=100 MeV).

The original E859 Phoswich Array consisted of 24 identical modules shaped like truncated pyramids with a focus at 60 cm and subtending a solid angle of approximately 6 msr. The modules were packaged into four sub–arrays of 2 horizontally by 3 vertically which surround the target on the side of the beam opposite the E802 Spectrometer. The four sub–arrays cover a polar angular range from 50.2° to 129.8° ($|\eta| \leq$0.76) and an azimuthal range of $\Delta\phi \simeq$24°. Protons with a kinetic energy greater than 200 MeV will punch through the active plastic depth of the individual phoswich telescopes (0.5 cm plus 26.0 cm). With careful calibrations,

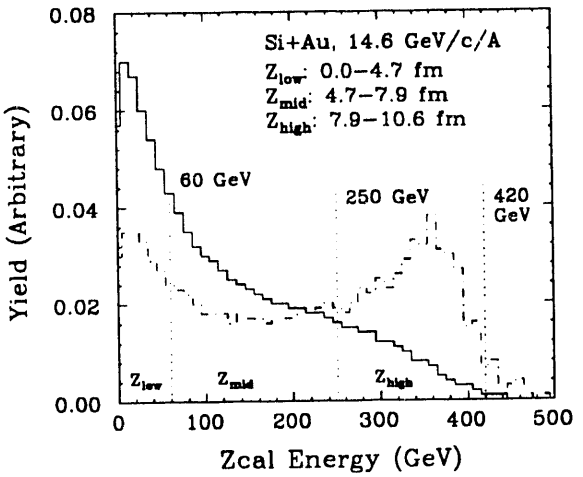

Fig. 2: The ZCAL energy distribution for minimum bias interaction triggers with a valid hit in the Phoswich Array (dashed) and PHOS hardware interaction triggers which require a valid hit in the Phoswich Array (solid). The dotted lines represent the ZCAL energy bins for defining the three impact parameter intervals, Z_{low}, Z_{mid} and Z_{high}.

however, particle identification is possible for kinetic energies up to 230–250 MeV.

Although each module in the original array subtended approximately 6 msr, the occupancy at the most forward angles in central ^{28}Si +^{197}Au collisions was too high for reliable PID (~25%). Therefore, the modules in the most forward sub–array were cut into identical quarters and repackaged with four new PMTs (a total of 24 new *quartered* modules) to fit within the original sub–array mount. All of the ^{28}Si +^{197}Au data presented here were acquired with the full 42–module array. In addition, all of the preliminary central ^{197}Au +^{197}Au data was taken with this high density sub–array by systematically substituting it for the other three sub–arrays. Even at backward angles the hit density for central ^{197}Au +^{197}Au collisions was too high for the large 6 msr modules.

Finally, the acceptance of the Phoswich Array was designed to have some overlap with the E802 Spectrometer. At the most forward angles we can compare the inclusive proton and deuteron kinetic energy spectra with those measured by the Spectrometer. The comparion is shown in Fig. 1 for minimum bias triggers at a laboratory angle of 50°.

3. Preliminary ^{28}Si +^{197}Au Results

In order to study the centrality dependence of proton and deuteron emission in 14.6 A·GeV/c ^{28}Si +^{197}Au collisions, we generated spectra according to constraints on the collision impact parameter. Impact parameter selection is accomplished by placing software constraints on the projectile spectator energy measured in the Zero Degree Calorimeter (ZCAL). To ensure adequate statistics in each spectrum, we defined three impact parameter intervals (or three ZCAL energy bins). The ZCAL energy bins and the corresponding impact parameter intervals (calculated using a simple overlapping spheres geometry for the nuclei) are shown in Fig. 2. The dashed and solid histograms represent the energy distribution in ZCAL for minimum bias interaction triggers (dashed) and interaction triggers in which there

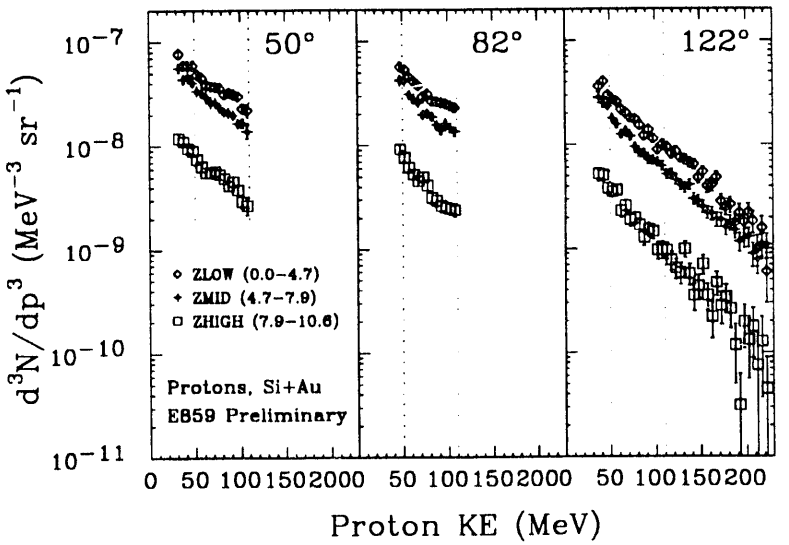

Fig. 3: Acceptance–corrected ^{28}Si +^{197}Au proton momentum density distributions as a function of impact parameter interval for three measured laboratory angles.

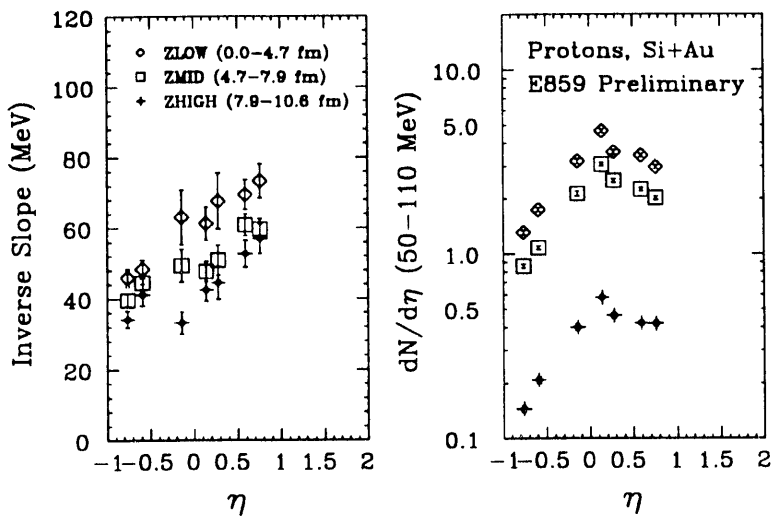

Fig. 4: The inverse slope parameters and corresponding pseudo–rapidity density distributions from exponential fits of the ^{28}Si +^{197}Au proton kinetic energy spectra between 50 and 110 MeV as a function of impact parameter interval and pseudo–rapidity.

was at least one hit in the phoswich array (a phoswich hardware trigger). The three ZCAL energy bins, Z_{low} (0–60 GeV), Z_{mid} (60–250 GeV) and Z_{high} (250–420 GeV) correspond to the impact parameter intervals 0.0–4.7 fm, 4.7–7.9 fm and 7.9–10.6 fm, respectively.

Fig. 3 shows the acceptance–corrected proton momentum density distribution as a function of kinetic energy for each of the ZCAL energy bins at three different laboratory angles. At the more backward angles, PID is possible for the full dynamic range of the detector modules (over 200 MeV). At more forward angles, the hit density effectively limits unambiguous

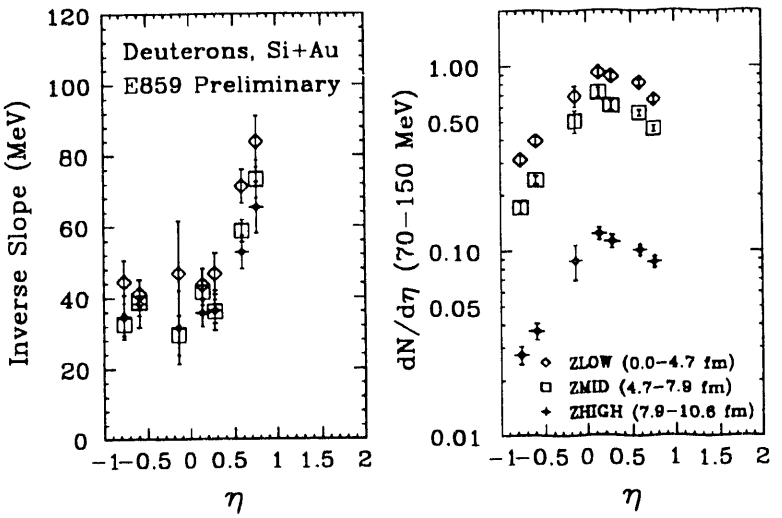

Fig. 5: The inverse slope parameters and corresponding pseudo–rapidity density distributions from exponential fits of the ^{28}Si +^{197}Au deuteron kinetic energy spectra between 70 and 150 MeV as a function of impact parameter interval and pseudo–rapidity.

PID to approximately 110 MeV (in ΔE–E space, multiple minimum ionizing pions obscure the proton band at higher energies). The low energy thresholds are determined primarily by target absorption (note that the threshold at 82° is considerably higher than at 50° or 122°).

For consistency, we have fit the proton and deuteron spectra with a simple exponential in kinetic energy (a Boltzmann distribution) over a fixed kinetic energy interval for all angles (or η). The proton kinetic energy interval, 50 to 110 MeV, is shown in Fig. 3 by the vertical dotted lines. The corresponding deuteron interval is 70 to 150 MeV. The inverse slope parameters from the fits to the proton spectra are shown in the left hand panel of Fig. 4 as a function of pseudo–rapidity and impact parameter interval. The slope parameters indicate the expected centrality dependence; harder spectra (or higher *"temperatures"*) for more central collisions. The pseudo–rapidity density distributions obtained by integrating the data between 50 and 110 MeV (denoted as $dN/d\eta$(50–110 MeV)) are shown in the right hand panel of Fig. 4. The shapes show little dependence on the impact parameter interval and the peaks appear to be at similar values of η (approximately 0.2–0.3 units). This indicates that the protons come primarily from a target–like source. There is also an order of magnitude difference in yield between the most central (Z_{low}) and the most peripheral (Z_{high}) impact parameters (see the left hand panel of Fig. 6).

The behavior of the deuterons mirrors that of the protons. The inverse slope parameters and pseudo–rapidity density distributions ($dN/d\eta$(70–150 MeV)) are shown in Fig. 5 as a function of pseudo–rapidity and impact parameter interval. Again, the shapes of the pseudo–rapidity density distributions appear to be independent of impact parameter. Indeed, the shapes and the peak η values of the distributions, as well as the relative yield as a function of the impact parameter are all virtually identical to those in Fig. 4. The similarity between the protons and deuterons is further demonstrated in Fig. 6. The left hand panel of the figure shows the impact parameter constrained yields of both protons and deuterons relative to the

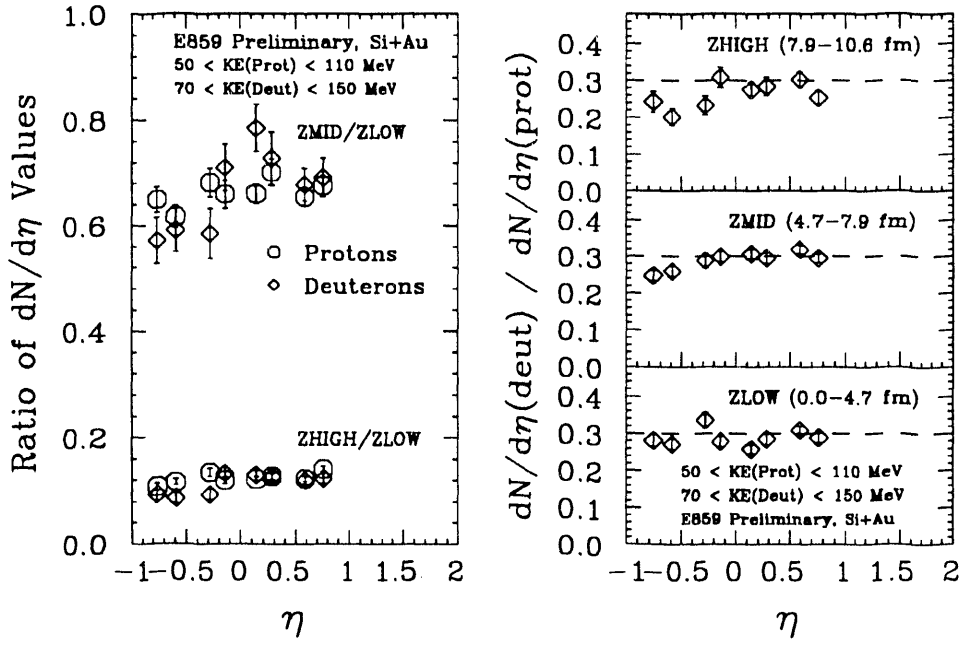

Fig. 6: The pseudo–rapidity dependence of the impact parameter constrained proton and deuteron yields relative to the yield of the most central impact parameter (left hand panel). Also shown is the relative yield of deuterons to protons as a function of impact parameter interval and pseudo–rapidity (right hand panel). The dashed lines are to aid in the comparison among the impact parameter intervals.

yield at the most central impact parameter (Z_{mid}/Z_{low} and Z_{high}/Z_{low} ratios of $dN/d\eta$) as a function of η. The centrality and pseudo–rapidity dependence of the proton and deuteron yields are virtually identical (although the ratios tend to decrease for the deuterons at the most backward angles). The right hand panel of Fig. 6 shows the deuteron yield relative to the proton yield as a function of pseudo–rapidity and centrality. Within the kinetic energy intervals used to generate the $dN/d\eta$, the deuteron yield is virtually a fixed fraction of the proton yield independent of pseudo–rapidity and centrality. Only slight deviations appear at the most backward angles.

4. Preliminary ^{197}Au +^{197}Au Results

The hit density in the E859 Phoswich Array increased by approximately a factor of three when the beam was changed to 11.7 A·GeV/c ^{197}Au . The increased hit density limited the information available from the full array. Central collisions completely saturated the high density (24 quartered modules) sub–array at the most forward angles; the data for minimum bias triggers, however, looked very similar to central ^{28}Si +^{197}Au . Therefore, only minimum bias triggers were acquired with the full E859 Phoswich Array. To study central collisions, the high density sub–array was systematically substituted for each of the other three sub–arrays and approximately 100k central triggers were acquired at each location.

Fig. 7 shows preliminary acceptance–corrected ^{197}Au +^{197}Au proton momentum density distributions for both minimum bias and central triggers. The central hardware trigger for the ^{197}Au beam data was based on a lack of energy in the ZCAL; a multiplicity–based central

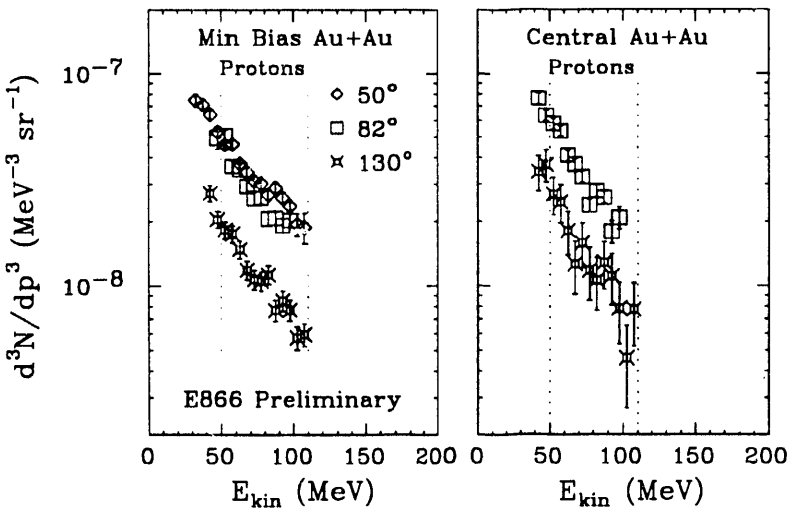

Fig. 7: Acceptance–corrected ^{197}Au +^{197}Au proton momentum density distributions for both minimum bias and central collisions at three different laboratory angles.

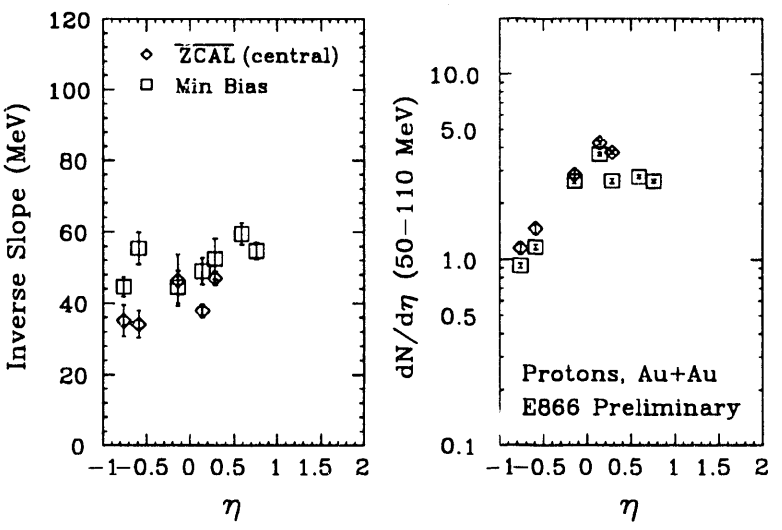

Fig. 8: The inverse slope parameters and corresponding pseudo–rapidity density distributions from exponential fits of the ^{197}Au +^{197}Au proton kinetic energy spectra between 50 and 110 MeV for both minimum bias and central collisions as a function of pseudo–rapidity.

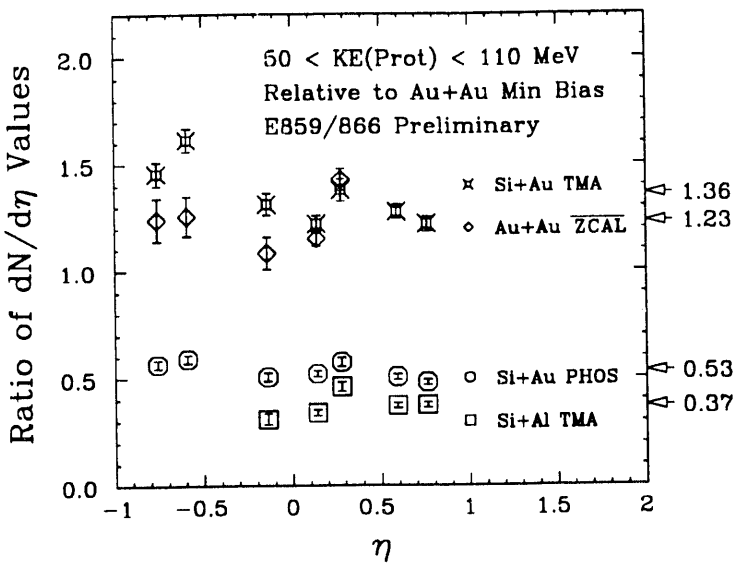

Fig. 9: The values of $dN/d\eta$(50–110 MeV) relative to minimum bias ^{197}Au +^{197}Au for various triggers as a function of pseudo–rapidity. The mean value over all η for each system–trigger is shown by the arrow on the right hand side of the figure.

trigger could not be formed with the E859 apparatus. For the Phoswich Array data, the ZCAL central trigger, denoted $\overline{ZCAL}$, represented approximately 7.4% of the target–out corrected interaction rate. This corresponds to an impact parameter range of approximately 0.0–3.7 fm (the square root of $0.074 \times b^2_{max}$, where b_{max} is simply the diameter of a ^{197}Au nucleus). Positive proton identification is again limited to a kinetic energy interval of 50 to 110 MeV; the deuteron sample is statistically unsuitable for analysis. The spectra have been fit with an exponential in kinetic energy and the inverse slope parameters and data-integrated $dN/d\eta$(50–110 MeV) are shown in Fig. 8.

Perhaps the most striking feature of Fig. 8 is the similarity between the data for the two hardware triggers (the similarity is apparent in Fig. 7 as well). The pseudo–rapidity density distributions are virtually identical while the slope parameters show only a weak dependence on η and little difference between the two triggers. Although there is no data for central triggers at the most forward angles, it appears that the peaks of the $dN/d\eta$ distributions are very close to those for the ^{28}Si +^{197}Au data (see Fig. 4). The rather unintuitive behavior of the ^{197}Au beam proton data can not, at present, be explained.

A summary and comparison of the ^{28}Si +^{197}Au and ^{197}Au +^{197}Au proton data is given in Fig. 9. Here, the values of $dN/d\eta$(50–110 MeV) relative to minimum bias ^{197}Au +^{197}Au are shown for various triggers as a function of η. The value of this ratio appears to be fairly constant as a function of pseudo–rapidity for each system–trigger (the ^{28}Si +^{197}Au TMA trigger is a multiplicity–based central hardware trigger which typically represents 7% of the raw interaction rate; PHOS is simply a minimum bias interaction trigger). The mean value of the ratio over all η and for each system–trigger is shown by the arrows on the right hand side of the figure. What is perhaps most remarkable is that the proton yield for central ^{28}Si +^{197}Au is larger than for central ^{197}Au +^{197}Au (note that both the TMA and $\overline{ZCAL}$ central

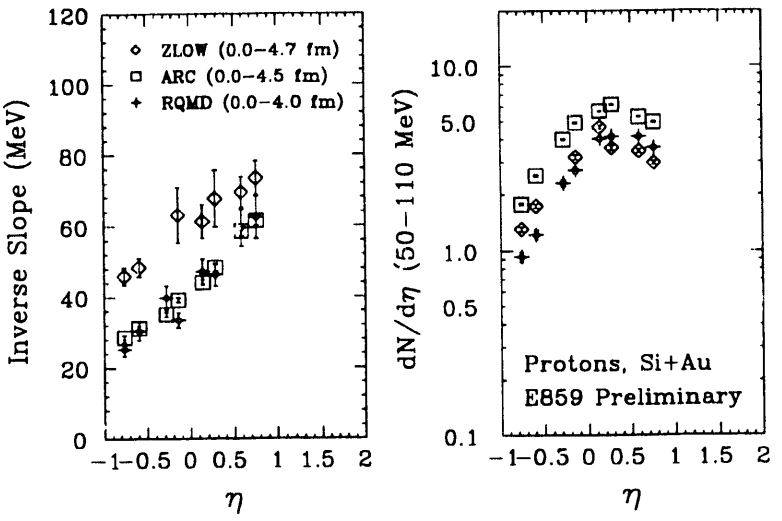

Fig. 10: A comparison of the ^{28}Si $+^{197}$Au proton (Z_{low}) slope parameters and pseudo–rapidity density distributions with the ARC and RQMD calculations.

triggers select virtually the same fraction of the raw interaction rate).

4. Model Comparisons

In this section we will compare the inverse slope parameters and pseudo–rapidity density distributions to the relevant predictions of the ARC and RQMD models for protons. In order to produce a valid comparison, the output of both models will be treated exactly like the data. This means that the calculated proton kinetic energy spectra will be fit over the same kinetic energy interval as the data (50 to 110 MeV). The integration of the data for the pseudo–rapidity density distributions will also be restricted to this same interval. Since the Phoswich Array data have been fully acceptance–corrected, the only other requirements placed on the model calculations will be a range of impact parameters which correspond, as nearly as possible, to the range estimated for the data.

The comparisons for the ^{28}Si $+^{197}$Au reaction will be done with existing ARC and RQMD event sets. The ARC event set contains randomly selected impact parameters in the range 0.0–4.5 fm; the range of impact parameters for the RQMD event sample is 0.0–4.0 fm. Both of these impact parameter intervals correspond reasonably well with the Z_{low} constraint on the measured ZCAL energy. The comparison of the inverse slope parameters and pseudo–rapidity density distributions with the Z_{low} proton data is shown in Fig. 10. Both the ARC and RQMD slope parameters are systematically low compared to the data indicating that the calculated proton spectra over this kinetic energy interval and at these pseudo–rapidities are too steep. Indeed, between 50 and 110 MeV, ARC and RQMD both produce a two–component spectrum and the fitted slope parameters reflect the influence of the lower temperature component. However, the integrated yields (recall that the integration does not rely on the slope fits) between 50 and 110 MeV agree reasonably well with the data. Even the shapes of the $dN/d\eta$ distributions are all remarkably similar. We should caution though that neither the ARC nor the RQMD event sets contain deuterons which account for

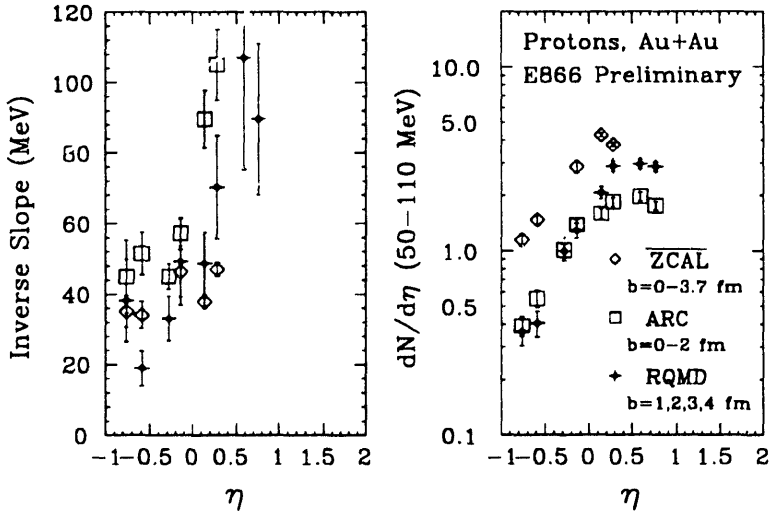

Fig. 11: A comparison of the ^{197}Au +^{197}Au central ($\overline{ZCAL}$) proton slope parameters and pseudo–rapidity density distributions with the ARC and RQMD calculations.

approximately 30% of the protons detected in the Phoswich Array (see Fig. 6).

The ^{197}Au beam results have also been compared with existing ARC and RQMD event sets. As has been pointed out, the $\overline{ZCAL}$ trigger represents an impact parameter range of approximately 0.0–3.7 fm. Unfortunately, the impact parameter interval available with existing ARC events is 0.0–2.0 fm and the statistics are limited. However, the situation is considerably better with RQMD. Here, four separate event sets are available with fixed impact parameters of 1.0, 2.0, 3.0 and 4.0 fm. The data from each RQMD impact parameter have been appropriately weighted to form a single set of proton spectra which essentially correspond to an impact parameter range of 0.0–4.0 fm.

Fig. 11 shows the comparison of the inverse slope parameters and the corresponding pseudo–rapidity density distributions for the $\overline{ZCAL}$ triggered data and the ARC and RQMD calculations. Although the RQMD spectra have been treated just like the data, the fit to the ARC spectra have not been restricted to the interval 50–110 MeV (due to the poor statistics). At back angles (negative η), the slope parameters all agree fairly well. However, at more forward angles, both calculations show a dramatic increase in the slope parameter; the ARC values for the two most forward angles are greater than 120 MeV. Although there is no central proton data at the most forward angles, the trend of the measured slope parameters does not suggest such a drastic increase with η.

The $dN/d\eta$ values shown in the right hand panel of Fig. 11 are integrals of the data over the restricted kinetic energy interval. The shapes of both the ARC and RQMD pseudo-rapidity density distributions do not agree with the data. They appear to be peaked at higher values of η and the tails of the distributions (at backward angles) are much steeper. Any discrepancy between impact parameter intervals will certainly affect the overall proton yields and the lack of deuterons in both ARC and RQMD would tend to produce an excess of protons. However, it is unlikely that such discrepancies will affect the shapes of the distribution since the colliding system is symmetric.

The ARC and RQMD calculations clearly agree much better with the $^{28}Si + ^{197}Au$ data. This may simply reflect a better match between impact parameter intervals and superior statistics. However, the differences between the calculations and the ^{197}Au beam proton data appear to be more fundamental in that the shapes of the $dN/d\eta$ distributions do not appear to agree. Complete coverage with the upgraded E866 Phoswich Array and better statistics will certainly allow a more thorough comparison in the near future.

5. Acknowledgements

This work was performed under the auspices of the U.S. Department of Energy by the Lawrence Livermore National Laboratory under contract W-7405-ENG-48. Experiment 802 is supported in part by the U.S. Department of Energy under contracts and grants with Argonne National Laboratory, Brookhaven National Laboratory, UC-Berkeley, UC-Riverside, Columbia University and the Massechusetts Institute of Technology, and in part by NASA under contract with UC-Berkeley and by the US-Japan High Energy Physics Collaboration treaty.

6. References

1. Y. Pang *et al.*, Nucl. Phys. **A544**, 435c (1992); Phys. Rev. Lett. **68**, 2743 (1992).
2. H. Sorge *et al.*, Ann. Phys. (N.Y.) 192, 266 (1989); Nucl. Phys. **A498**, 567c (1989); Z. Phys. **C47**, 629 (1990).
3. T. Abbott *et al.*, Nucl. Instr. Meth. **A290**, 41 (1990).
4. T. Abbott *et al.*, Phys. Rev. Lett. **64**, 847 (1990); Phys. Rev. **D45**, 3906 (1992); Nucl. Phys. **A544**, 237c (1992).
5. Y. Akiba *et al.*, Nucl. Phys. **A544**, 445c (1992); Nucl. Phys. **A544**, 553c (1992).
6. J. B. Costales *et al.*, Nucl. Instr. and Meth., to be published.
7. D. H. Wilkinson, Rev. Sci. Instr. **23**, 414 (1952).

DATE
FILMED
11/23/93
END